



# LINC01094 Predicts Poor Prognosis in Patients With Gastric Cancer and is Correlated With EMT and Macrophage Infiltration

Technology in Cancer Research & Treatment  
Volume 21: 1-13  
© The Author(s) 2022  
Article reuse guidelines:  
sagepub.com/journals-permissions  
DOI: 10.1177/15330338221080977  
journals.sagepub.com/home/tct  


Yuanchun Ye, MD<sup>1,2,\*</sup> , Ouyang Ge, MD<sup>3,\*</sup>, Chuanbing Zang, PhD<sup>2</sup>,  
Leina Yu, MD<sup>2</sup>, Jan Eucker, MD<sup>2</sup>, and Yuling Chen, MD<sup>4</sup>

## Abstract

**Objectives:** The novel long non-coding RNA (lncRNA) LINC01094 is often upregulated in renal cell carcinoma and glioma; however, its role in gastric cancer remains unclear. Here, we aim to demonstrate the relationship between LINC01094 and gastric cancer. **Method:** The gene expression (RNASeq) data of 375 patients with localized, locally advanced, and metastatic gastric cancer were extracted from The Cancer Genome Atlas. The Kruskal–Wallis test, Wilcoxon signed-rank test, and logistic regression were used to analyze the relationship between the clinicopathological characteristics and LINC01094 expression. Cox regression analysis and the Kaplan–Meier method were used to assess prognostic factors of gastric cancer. A nomogram based on Cox multivariate analysis was used to predict the impact of LINC01094 on gastric cancer prognosis. Gene set enrichment analysis (GSEA) was used to identify key LINC01094-associated signaling pathways. Fluorescence in situ hybridization (FISH) was performed to detect the location of LINC01094 in the tissue, and a competing endogenous (ce)RNA network was constructed to identify LINC01094-related genes. Spearman’s rank correlation was used to elucidate the association between LINC01094 expression level and immune cell infiltration level. **Result:** LINC01094 expression was upregulated in gastric cancer tissues and strongly associated with overall survival using univariate Cox regression (hazard ratio [HR] = 1.476, 95% CI = 1.060–2.054,  $P = .021$ ) and multivariate Cox regression analysis (HR = 1.535, 95% CI = 1.021–2.308,  $P = .039$ ). The area under the receiver operating characteristic curve of LINC01094 was 0.910. GSEA showed a strong relationship between LINC01094 and the epithelial-mesenchymal transition pathway. RNA-FISH demonstrated that LINC01094 localized in the cytoplasm. It was closely related to the epithelial-mesenchymal transition (EMT) marker *SNAI2*, according to ceRNA ( $R = 0.61$ ,  $P < .001$ ), and macrophage-related gene *FCGR2A*. Macrophages were also significantly positively correlated with LINC01094 expression ( $R = 0.747$ ,  $P < .001$ ). **Conclusion:** High LINC01094 expression predicts poor prognosis in gastric cancer and is correlated with the epithelial-mesenchymal transition pathway and macrophage infiltration.

## Keywords

gastric cancer, long non-coding RNA, bioinformatics, immunity, TCGA

<sup>1</sup> Department of Gastroenterology, Quanzhou First Hospital affiliated to Fujian Medical University, Quanzhou, Fujian Province, People’s Republic of China

<sup>2</sup> Department of Hematology Oncology and Tumor Immunity, Benjamin Franklin Campus, Charité–Universitätsmedizin Berlin, Corporate Member of Freie Universität Berlin, Humboldt-Universität zu Berlin, Berlin, Germany

<sup>3</sup> Institute for Experimental Endocrinology, Charité–Universitätsmedizin Berlin, Corporate Member of Freie Universität Berlin, Humboldt-Universität zu Berlin, Berlin, Germany

<sup>4</sup> Department of Rheumatology and Immunology, The Seventh Affiliated Hospital Sun Yat-sen University, Shenzhen, Guangdong Province, People’s Republic of China

\*Yuanchun Ye and Ouyang Ge contributed equally to this paper.

## Corresponding Authors:

Jan Eucker, Department of Hematology Oncology and Tumor Immunity, Benjamin Franklin Campus, Charité–Universitätsmedizin Berlin, Corporate Member of Freie Universität Berlin, Humboldt-Universität zu Berlin, Hindenburgdamm 30, 12203 Berlin, Germany.

Email: Jan.eucker@charite.de

Yuling Chen, Department of Rheumatology, The Seventh Affiliated Hospital Sun Yat-sen University, Shenzhen, Guangdong Province, People’s Republic of China.

Email: anky6750119@163.com



Creative Commons Non Commercial CC BY-NC: This article is distributed under the terms of the Creative Commons Attribution-NonCommercial 4.0 License (<https://creativecommons.org/licenses/by-nc/4.0/>) which permits non-commercial use, reproduction and distribution of the work without further permission provided the original work is attributed as specified on the SAGE and Open Access page (<https://us.sagepub.com/en-us/nam/open-access-at-sage>).

## Abbreviations

ACC, adrenocortical carcinoma; BP, biological process; BRCA, breast invasive carcinoma; CC, cellular component; ceRNA, competing endogenous RNA; CHOL, cholangiocarcinoma; CI, confidence interval; COAD, colon adenocarcinoma; DC, dendritic cell; DEGs, differentially expressed genes; EMT, epithelial to mesenchymal transition; ESCA, esophageal carcinoma; FAO, fatty acid oxidation; FISH, fluorescence in situ hybridization; GC, gastric cancer; GO, gene ontology; GSEA, gene set enrichment analysis; HR, hazard ratio; KEGG, Kyoto encyclopedia of genes and genomes; lncRNA, long noncoding RNA; MESO, mesothelioma; MF, molecular function; OS, overall survival; PPI, protein-protein interaction; READ, rectum adenocarcinoma; ROC, receiver operating characteristic; ssGSEA, single-sample GSEA; STAD, stomach adenocarcinoma; TAM, tumor-associated macrophage; TCGA, The Cancer Genome Atlas; TME, tumor microenvironment; TPM, transcripts per million; UCS, uterine carcinosarcoma.

Received: September 6, 2021; Revised: January 14, 2022; Accepted: January 28, 2022.

## Introduction

Gastric cancer (GC) is the fifth most common cancer globally and is responsible for 8.2% of all deaths associated with cancer, thereby making it the third leading cause of cancer death worldwide.<sup>1</sup> Even though the five-year relative survival rate increased to 32% during 2010 to 2016,<sup>2</sup> the prognosis remains poor and treatment options of GC patients are limited. Abnormal expression of genes, such as *CDH1*, *APC*, *BRCA2*, *MLH1*, and *IRF6*, is closely associated with tumorigenesis and prognosis of patients with GC.<sup>3–8</sup> Currently, the clinical values of the most reported prognostic markers are limited and there is a need for more accurate prognostic markers.

Long non-coding RNAs (lncRNAs) are non-coding RNAs longer than 200 nucleotides.<sup>9</sup> Recent integrative genomic studies have shown that lncRNAs play a key role in the development of cancer.<sup>10–13</sup> Although a small number of lncRNAs have been extensively studied, myriad members of this class remain functionally uncharacterized. Increasing evidence suggests that lncRNAs may mediate oncogenic or tumor-suppressing effects and can become new targets for cancer treatment.<sup>12,14</sup>

The novel long intergenic nonprotein coding RNA LINC01094, which affiliates with the lncRNA class located on chromosome 4, is upregulated in clear cell renal cell carcinoma and glioma.<sup>15,16</sup> Overexpression of LINC01094 closely correlates with the progression of cancer and radioresistance in cancer treatment.<sup>17</sup> However, there has been limited research on the association between LINC01094 and cancer, including GC.

In this study, we explored the correlation between LINC01094 and GC. The Cancer Genome Atlas (TCGA) database was used to analyze the association between LINC01094 expression, clinicopathological features, and tumor-infiltrating immune cells. Gene set enrichment analysis (GSEA), protein-protein interaction (PPI), and competing endogenous RNA (ceRNA) network analysis were used to reveal the possible molecular functions of LINC01094 in GC. Our study revealed the potential roles of LINC01094 in GC prognosis and tumor immunology, which may facilitate the understanding of the mechanisms of gastric carcinogenesis.

## Materials and Methods

### Sample and Data Sets

TCGA and GTEx RNAseq data were downloaded in TPM format from the UCSC XENA database (<http://xenabrowser.net/datapages/>) and uniformly processed with the Toil process.<sup>18</sup> The gene expression data (HTSeq-FPKM and HTSeq-counts) with clinical information from the STAD project were retrospectively collected from TCGA database (<https://cancergenome.nih.gov/>),<sup>19</sup> and level 3 HTSeq-FPKM data were converted into TPM for subsequent analyses. Unavailable or unknown clinical features were considered as missing values. A curated set of clinical parameters was obtained from the TCGA Pan-Cancer Clinical Data Resource (TCGA-CDR).<sup>20</sup>

### Identification of Differentially Expressed Genes and Gene Function Analysis

According to the LINC01094 expression data (HTSeq-counts) from STAD, patients were divided into high- and low-expression groups. The median was used as a cutoff value for classification, and differentially expressed genes (DEGs) were analyzed using the DESeq2 package<sup>21</sup> on HTSeq-counts data.  $|\log_{2}FC| > 1.5$  and  $\text{padj} < 0.05$  were considered threshold values for DEGs.

Gene ontology (GO) functional analyses, including Cellular Component (CC), Molecular Function (MF), Biological Processes (BP), and Kyoto Encyclopedia of Genes and Genomes (KEGG) pathway enrichment analyses, were performed on DEGs using the clusterProfiler package<sup>22</sup> in R (version 3.6.2) with *P* values adjusted by the Benjamini and Hochberg method.

### Gene Set Enrichment Analysis (GSEA)

In the present study, GSEA was performed using the clusterProfiler package in R to elucidate the significant function and pathway differences between high- and low-expression LINC01094 groups.<sup>23</sup> The expression level of LINC01094 was used as a phenotype label. The number of gene set

permutations was 1000 for each analysis. The pathway enrichment was analyzed based on  $|\text{NES}| > 1$ ,  $p.\text{adj} < 0.05$ , and  $\text{FDR} < 0.25$ .

### The Immune Infiltration Analysis by ssGSEA

Data on the marker gene of 24 immune cells were obtained from an immunity study,<sup>24</sup> and the infiltration of 24 immune cells within the GC sample from TCGA was analyzed by single-sample GSEA (ssGSEA) using the GSVA package<sup>25</sup> in R. Moreover, the correlations between LINC01094 and these 24 cell types were analyzed using Spearman's rank correlation.

### Protein–Protein Interaction Analysis

The Search Tool for the Retrieval of Interacting Genes (<http://string-db.org>, version 11.0) online database was used to predict the PPI network of co-regulated hub genes and to analyze the functional interactions between proteins.<sup>26</sup> An interaction with a combined score of  $>0.7$  was considered statistically significant. To identify crucial subnetworks, data on the hub genes in the PPI network were extracted using MCODE,<sup>27</sup> and the Cytoscape software (version 3.7.2) was used to visualize the PPI network.<sup>28</sup> Functional enrichment analysis was performed using Metascape (<http://metascape.org/>).<sup>29</sup>

### RNA-FISH

To further explore the underlying mechanisms of LINC01094-mediated effects, fluorescence in-situ hybridization (FISH) was performed to detect the location of lincRNA in tissue. The human gastric adenocarcinoma tissue microarrays, purchased from Outdu Biotech Company (Shanghai, China), contained 15 gastric adenocarcinoma tissues and paired normal gastric tissues. The RNA-FISH assay was carried out according to previous studies.<sup>30</sup> The RNA probe was 5'-TGCACAACCTGGTTTGTAAGTCTGAAGATCCCCTG-3'.

### ceRNA

The LINC01094-associated ceRNA network was constructed based on the "ceRNA hypothesis."<sup>31</sup> The StarBase database was used to predict the miRNA-lincRNA regulatory relationships.<sup>32</sup> The mRNA target genes from the predicted miRNA were selected from multiple microRNA-target databases, including miRecords, miRTarBase, and TarBase, using the multiMIR package in R.<sup>33</sup> Of the selected mRNAs, those intersecting with the DEGs were used to construct the ceRNA in cytoscape software.<sup>28</sup> Gene enrichment analysis was performed with Metascape (<http://metascape.org/>).<sup>29</sup> The correlation between LINC01094 and the associated genes were analyzed using Spearman's rank correlation performed with the ggstats-plot package in R.<sup>34</sup> TIMER (<http://timer.cistrome.org/>) was performed to analyze the gene expression and macrophage

using partial Spearman's correlation.<sup>35</sup> The proportions of immune cell infiltration were calculated with CIBERSORT-ABS,<sup>36</sup> MCPOUNTER,<sup>37</sup> and EPIC.<sup>38</sup>

### Statistical Analysis

All statistical data and plots were generated using the R program (version 3.6.2). The Wilcoxon rank-sum test and Wilcoxon signed-rank test were used to analyze the expression of LINC01094 in nonpaired and paired samples, respectively. The Kruskal–Wallis test, Wilcoxon signed-rank test, and logistic regression were used to evaluate the relationship between clinical variables and the expression of LINC01094. Cox regression analysis and the Kaplan–Meier method were used to evaluate prognostic factors. Multiple Cox analysis was used to compare the expression of LINC01094 with other clinical traits. All tests were two tailed, and  $P < .05$  was considered statistically significant. Receiver operating characteristic (ROC) analysis for binary assessment was performed using the pROC package.<sup>39</sup> Multivariate Cox regression analysis was used to determine the optimal model, and a nomogram was constructed to predict the prognosis of GC patients using the rms package in R.

## Results

Table 1 shows the clinical information from TCGA of the GC patients whose data were used in this study, including TNM stage, pathologic stage, primary therapy outcome, sex, race, tumor location, and treatment. A total of 241 (64.3%) male patients and 134 (35.7%) female patients were analyzed, including 238 (73.7%) White patients, 74 (22.9%) Asian patients, and 11 (3.4%) patients of other races. The median age of the diagnosed patients was 67 years, and 19 (5%) patients had tumors classified as T1, 80 (21.3%) as T2, 168 (45%) as T3, and 100 (26%) as T4. The number of patients without lymph node involvement (N0) was 111 (31.1%), with N1 was 97 (27.2%), with N2 was 75 (21.0%), and with N3 was 74 (20.7%). In 330 patients, no metastatic disease was present (M0) (93.0%), and metastatic cancer was diagnosed in 25 patients (M1: 7.0%). Stage I disease was identified in 53 patients (15.1%), stage II in 111 patients (31.5%), stage III in 150 patients (42.6%), and stage IV in 38 patients (10.8%). Some patients had a history of reflux (18.2%), received antireflux treatment (20.7%), or had Barrett's esophagus (7.2%). Moreover, the expression level of LINC01094 was highly related to histological type ( $P = .001$ ), histologic grade ( $P < .001$ ), and anatomic neoplasm subdivision ( $P = .048$ ).

As shown in Figure 1A, a significant difference in gene expression between normal and tumor tissues was found in most types of cancer, including GC. LINC01094 expression levels in non-paired and paired tumors were markedly higher than those in normal tissues (Figure 1B to C). To identify the diagnostic value of LINC01094 in patients with GC, ROC curve analysis was performed. The area under the ROC curve

**Table 1.** Association Between LINC01094 and Clinicopathologies Features based on TCGA.

Characters	Level	Overall	Low expression of LINC01094	High expression of LINC01094	<i>P</i>
N		375	188	187	
T stage (%)	T1	19 (5.2%)	15 (8.0%)	4 (2.2%)	.063 <sup>a</sup>
	T2	80 (21.8%)	39 (20.7%)	41 (22.9%)	
	T3	168 (45.8%)	88 (46.8%)	80 (44.7%)	
	T4	100 (27.2%)	46 (24.5%)	54 (30.2%)	
N stage (%)	N0	111 (31.1%)	61 (33.5%)	50 (28.6%)	.459
	N1	97 (27.2%)	43 (23.6%)	54 (30.9%)	
	N2	75 (21.0%)	40 (22.0%)	35 (20.0%)	
	N3	74 (20.7%)	38 (20.9%)	36 (20.6%)	
M stage (%)	M0	330 (93.0%)	162 (92.6%)	168 (93.3%)	.942
	M1	25 (7.0%)	13 (7.4%)	12 (6.7%)	
Pathologic stage (%)	Stage I	53 (15.1%)	34 (19.0%)	19 (11.0%)	.171
	Stage II	111 (31.5%)	51 (28.5%)	60 (34.7%)	
	Stage III	150 (42.6%)	74 (41.3%)	76 (43.9%)	
	Stage IV	38 (10.8%)	20 (11.2%)	18 (10.4%)	
Primary therapy outcome (%)	CR	231 (72.9%)	120 (71.4%)	111 (74.5%)	.565 <sup>a</sup>
	PD	65 (20.5%)	38 (22.6%)	27 (18.1%)	
	PR	4 (1.3%)	1 (0.6%)	3 (2.0%)	
	SD	17 (5.4%)	9 (5.4%)	8 (5.4%)	
Gender (%)	Female	134 (35.7%)	71 (37.8%)	63 (33.7%)	.474
	Male	241 (64.3%)	117 (62.2%)	124 (66.3%)	
Race (%)	Asian	74 (22.9%)	41 (25.0%)	33 (20.8%)	.053 <sup>a</sup>
	Black or African American	11 (3.4%)	9 (5.5%)	2 (1.3%)	
	White	238 (73.7%)	114 (69.5%)	124 (78.0%)	
Histological type (%)	Diffuse type	63 (16.8%)	26 (13.8%)	37 (19.9%)	.001 <sup>a</sup>
	Mucinous type	19 (5.1%)	6 (3.2%)	13 (7.0%)	
	Not otherwise specified	207 (55.3%)	98 (52.1%)	109 (58.6%)	
	Papillary type	5 (1.3%)	5 (2.7%)	0 (0.0%)	
	Signet ring type	11 (2.9%)	6 (3.2%)	5 (2.7%)	
	Tubular type	69 (18.4%)	47 (25.0%)	22 (11.8%)	
Histologic grade (%)	G1	10 (2.7%)	6 (3.3%)	4 (2.2%)	<.001 <sup>a</sup>
	G2	137 (37.4%)	86 (47.3%)	51 (27.7%)	
	G3	219 (59.8%)	90 (49.5%)	129 (70.1%)	
Anatomic neoplasm subdivision (%)	Antrum/distal	138 (38.2%)	68 (37.2%)	70 (39.3%)	.048
	Cardia/proximal	48 (13.3%)	25 (13.7%)	23 (12.9%)	
	Fundus/body	130 (36.0%)	58 (31.7%)	72 (40.4%)	
	Gastroesophageal Junction	41 (11.4%)	29 (15.8%)	12 (6.7%)	
	Other	4 (1.1%)	3 (1.6%)	1 (0.6%)	
Reflux history (%)	No	175 (81.8%)	102 (81.6%)	73 (82.0%)	1
	Yes	39 (18.2%)	23 (18.4%)	16 (18.0%)	
Antireflux treatment (%)	No	142 (79.3%)	77 (77.0%)	65 (82.3%)	.496
	Yes	37 (20.7%)	23 (23.0%)	14 (17.7%)	
Barretts esophagus (%)	No	193 (92.8%)	118 (91.5%)	75 (94.9%)	.418 <sup>a</sup>
	Yes	15 (7.2%)	11 (8.5%)	4 (5.1%)	
Age (%)	< = 65	164 (44.2%)	84 (45.2%)	80 (43.2%)	.789
	>65	207 (55.8%)	102 (54.8%)	105 (56.8%)	
Age (median [IQR])		67.00 [58.00, 73.00]	67.00 [58.00, 72.00]	68.00 [58.00, 75.00]	.305 <sup>b</sup>

<sup>a</sup>Fisher exact test.<sup>b</sup>Nonnormal distribution.

of LINC01094 was 0.910 (95% confidence interval [CI] = 0.797-0.941), suggesting the potential diagnostic role of LINC01094 in GC (Figure 1D).

The correlations between LINC01094 expression and major clinicopathological factors, including T stage (T1, T2, and T3 vs T4, *P* = .019), histologic grade (G1 and G2 vs G3, *P* <

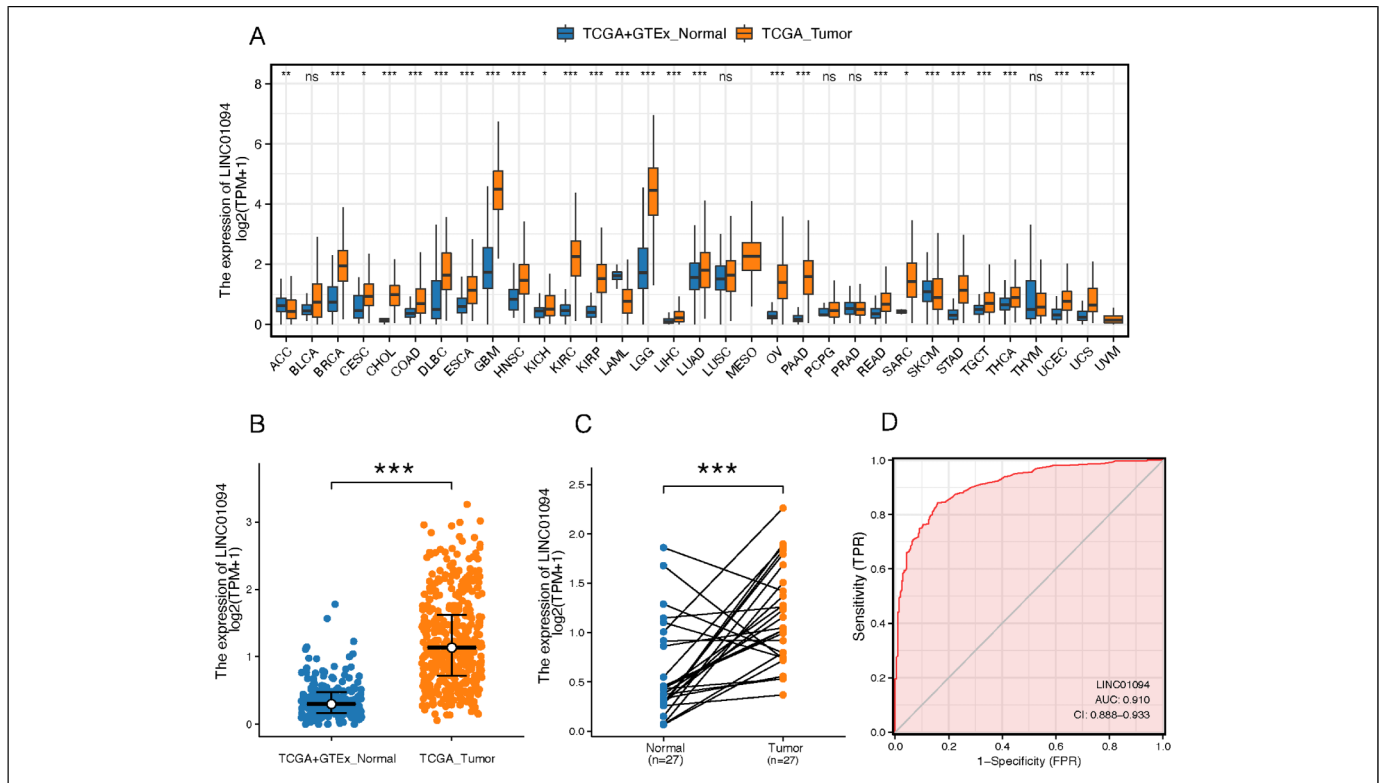


**Figure 1.** Expression levels of LINC01094 in 33 cancer tissues (A) and gastric cancer tissues (B) were analyzed by Wilcoxon rank-sum test using RNAseq data from TCGA and GTEX. Expression levels of LINC01094 in paired gastric cancer tissues and normal tissue samples from the same patients (C), analyzed by Wilcoxon signed-rank test, are shown. Expression level of LINC01094 is significantly higher in cancer tissues than normal samples. ROC analysis of LINC01094 expression shows a high ability to discriminate cancer tissues from normal samples (D). \*  $P < .05$ , \*\*  $P < .01$ , \*\*\*  $P < .001$ .

**Table 2.** LINC01094 Expression Associated With Clinical Pathological Characteristics (Logistic Regression).

Characteristics	Total (N)	Odds ratio (OR)	<i>P</i> value
T stage (T1 & T2 & T3 vs T4)	367	0.85 (0.74-0.97)	.019
N stage (N0 vs N1 & N2 & N3)	357	0.86 (0.73-1.00)	.060
M stage (M0 vs M1)	355	0.83 (0.69-1.02)	.059
Histologic grade (G1 & G2 vs G3)	366	0.73 (0.62-0.84)	<.001
Pathologic stage (Stage I & Stage II vs Stage III & Stage IV)	352	0.86 (0.74-0.99)	.039
Age (< = 65 vs > 65)	371	1.00 (0.88-1.12)	.969
Gender (female vs male)	375	1.07 (0.94-1.20)	.297
Primary therapy outcome (PD & SD & PR vs CR)	317	1.06 (0.89-1.25)	.478
Race (Asian & Black or African American vs White)	323	0.78 (0.63-0.93)	.009
Histological type (diffuse type & mucinous type & papillary type & Signet ring type vs tubular type)	167	1.81(1.35-2.53)	<.001
Anatomic neoplasm subdivision (antrum/distal vs fundus/body)	268	0.97 (0.84-1.12)	.664
Reflux history (no vs yes)	214	0.99 (0.75-1.34)	.943
Antireflux treatment (no vs yes)	179	1.17 (0.93-1.55)	.218
Barretts esophagus (no vs yes)	208	1.34 (0.82-2.53)	.300

.001), pathologic stage (stage I and stage II vs stage III and stage IV,  $P = .039$ ), race (Asian and Black or African American vs White,  $P = .009$ ), and histological type (diffuse, mucinous, papillary, and signature ring types vs tubular type,  $P < .001$ ) were determined using logistic regression, as shown in Table 2. High expression level of LINC01094 in GC was significantly associated with more advanced stage

(T4 vs T1, T2, and T3,  $P = .044$ ; Stage I vs II, III, or IV;  $P < .05$ ; G1 and G2 vs G3,  $P < .001$ ) (Figure 2A to C). This indicates that GC with higher expression of LINC01094 is likely to progress to a poorer pathological stage.

Univariate and multivariate Cox regression analyses were performed to investigate whether LINC01094 was an independent predictor of poor survival in GC patients, after excluding

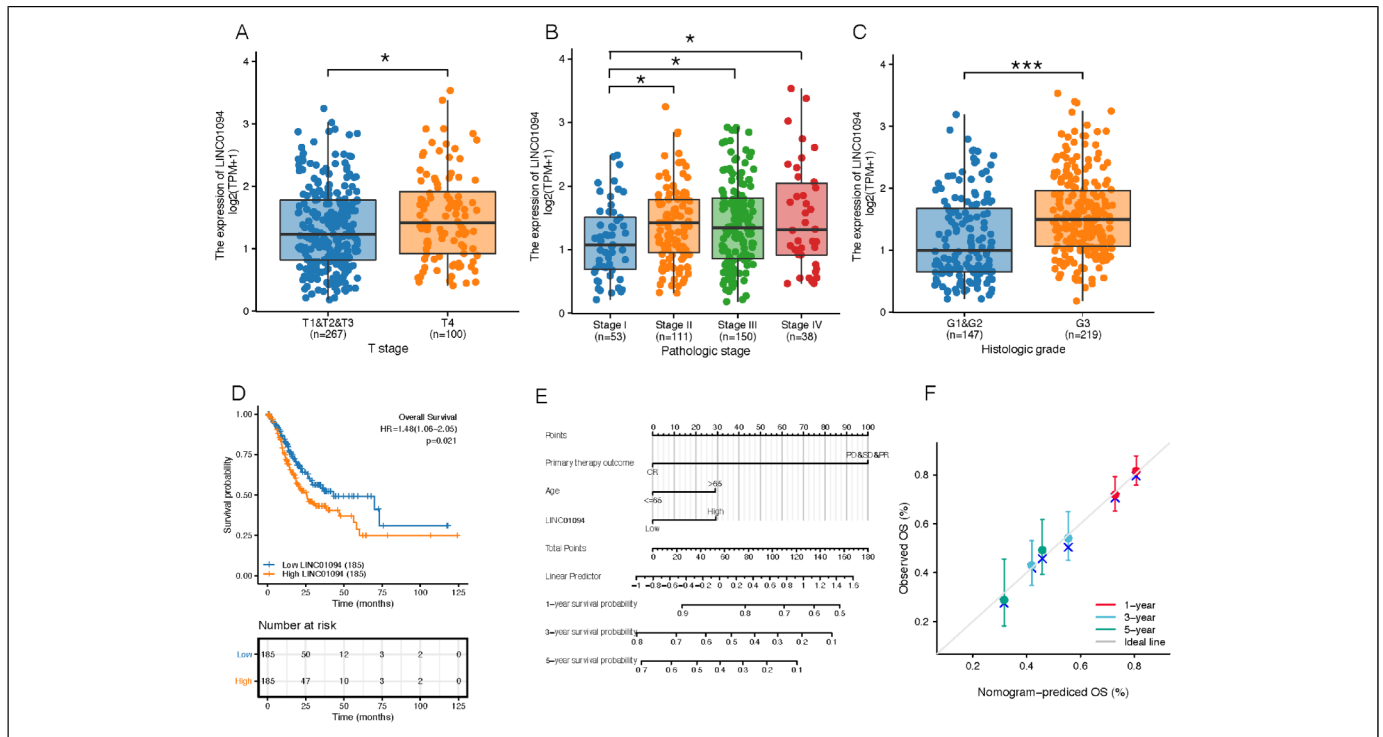


**Figure 2.** Association of LINC01094 expression and clinicopathological characteristics. (A) T stage, (B) pathologic stage, (C) histologic grade, (D) impact of LINC01094 expression on OS in GC patients in TCGA cohort, (E) nomogram for predicting the probability of 1-, 3-, 5-year OS for GC patients, and (F) calibration plot of the nomogram for predicting the probability of OS at 1, 3, 5 years. \*  $P < .05$ , \*\*  $P < .01$ , \*\*\*  $P < .001$ .

**Table 3.** Result of OS and Clinicopathologic Characteristics in GC Patients Using Univariate/Multivariate Analysis.

Characteristics	Total (N)	Univariate analysis		Multivariate analysis	
		HR (95% CI)	P value	HR (95% CI)	P value
T stage (T1 & T2 & T3 vs T4)	362	0.582 (0.383-0.884)	.011	0.732 (0.404-1.329)	.305
N stage (N0 vs N1 & N2 & N3)	352	0.519 (0.341-0.791)	.002	0.865 (0.443-1.690)	.672
M stage (M0 vs M1)	352	0.444 (0.255-0.772)	.004	0.868 (0.384-1.962)	.734
Histologic grade (G1 & G2 vs G3)	361	0.739 (0.522-1.045)	.087	0.663 (0.426-1.031)	.068
Pathologic stage (Stage I & Stage II vs Stage III & Stage IV)	347	0.514 (0.358-0.737)	<.001	0.788 (0.432-1.437)	.437
Histological type (diffuse type & mucinous type & papillary type & Signet ring type vs tubular type)	167	1.011 (0.613-1.667)	.967		
Age (< = 65 vs > 65)	367	0.617 (0.439-0.867)	.005	0.591 (0.391-0.893)	.013
Gender (female vs male)	370	0.789 (0.554-1.123)	.188		
Primary therapy outcome (PD & SD & PR vs CR)	313	4.228 (2.905-6.152)	<.001	4.313 (2.867-6.489)	<.001
Race (Asian & Black or African American vs White)	320	0.801 (0.515-1.247)	.326		
Anatomic neoplasm subdivision (Antrum/distal vs fundus/body)	267	1.037 (0.699-1.536)	.858		
Reflux history (no vs yes)	213	1.720 (0.861-3.436)	.125		
Antireflux treatment (no vs yes)	179	1.323 (0.739-2.368)	.346		
Barretts esophagus (no vs yes)	207	1.121 (0.410-3.069)	.824		
LINC01094 (high vs low)	370	1.476 (1.060-2.054)	.021	1.535 (1.021-2.308)	.039

patients with incomplete data. We included 370 GC patients for Cox regression analysis. Univariate Cox regression analysis revealed that LINC01094 closely correlated with overall

survival (OS) (hazard ratio [HR] = 1.535, 95% CI = 1.060-2.054,  $P = .021$ ) (Figure 2D). Moreover, other clinicopathological variables, including T stage (HR = 1.719, 95%

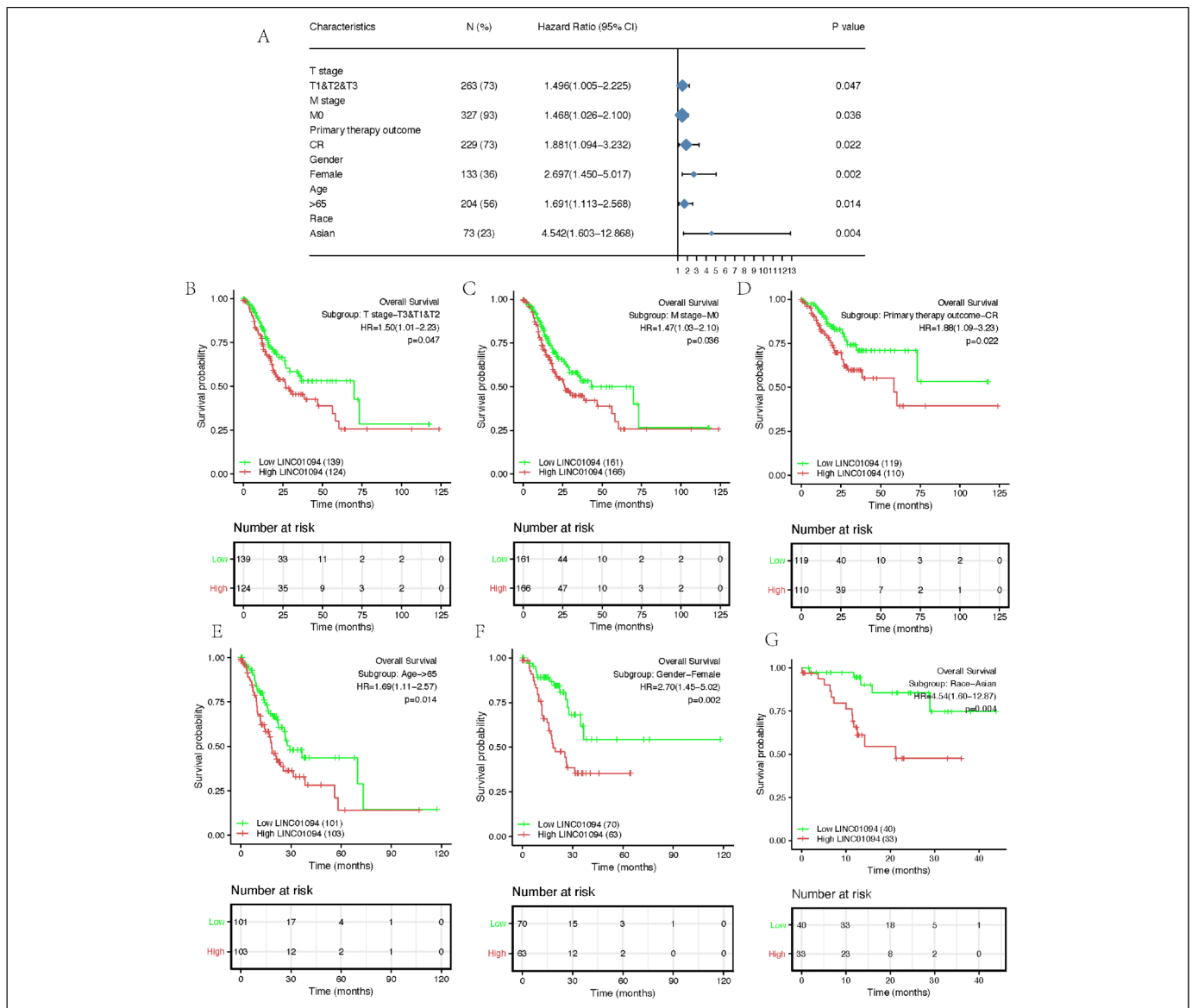


**Figure 3.** Forest plot of hazard ratios for the relationship between LINC01094 and OS (A). KM plots of OS between expression of LINC01094 and subgroups of GC patients (B-G). High level of LINC01094 is associated with poor survival outcomes in T1 & T2 & T3, M0, complete response (CR), Age >65, female, and Asian subgroups.

CI = 1.131-2.612,  $P = .011$ ), N stage (HR = 1.925, 95% CI = 1.264-2.931,  $P = .002$ ), distant metastasis (HR = 2.254, 95% CI = 1.295-3.924,  $P = .004$ ), pathologic stage (HR = 1.947, 95% CI = 1.358-2.793,  $P < .001$ ), primary therapy outcome (HR = 0.237, 95% CI = 0.163-0.344,  $P < .001$ ), and age (HR = 1.620, 95% CI = 1.154-2.276,  $P = .005$ ) were significantly related to OS. Variables with  $P < .1$  in univariate analysis were included in the multivariate Cox regression analysis; the primary therapy outcome (HR = 0.232, 95% CI = 0.154-0.349,  $P < .001$ ), age (HR = 1.693, 95% CI = 1.120-2.558,  $P = .013$ ), and LINC01094 (HR = 1.535, 95% CI = 1.021-2.308,  $P = .039$ ) were significantly related to OS (Table 3). These results indicate that LINC01094 is an independent indicator for predicting poor OS in GC patients.

As shown in Figure 3, the prognostic value of OS in each subgroup of GC patients was statistically significant in the T1, T2, T3 (HR = 1.496, 95% CI = 1.005-2.225,  $P = .047$ ), M0 (HR = 1.468, 95% CI = 1.026-2.100,  $P = .036$ ), complete response (HR = 1.881, 95% CI = 1.094-3.232,  $P = .022$ ), female (HR = 2.697, 95% CI = 1.450-5.017,  $P = .002$ ), age > 65 (HR = 1.691, 95% CI = 1.113-2.568,  $P = .014$ ), and Asian (HR = 4.542, 95% CI = 1.603-12.868,  $P = .004$ ) subgroups. High expression levels of LINC01094 were associated with poor survival outcomes in early-stage, elderly, female, and Asian patients with GC.

RNA-FISH revealed that the subcellular localization of LINC01094 was in the cytoplasm (Supplemental Figures 1 and 2). To elucidate the role of LINC01094 in GC, RNAseq



was performed to compare the gene expression in high- and low-LINC01094 expression groups. A total of 389 upregulated and downregulated genes were identified based on  $\text{padj} < 0.05$  and  $|\log\text{FC}| > 1.5$  (Figure 4A). The heat map showed the top 5 up and down co-expression genes (Figure 4B). GO functional enrichment analysis revealed changes in gene sets related to digestion, lipid digestion, triglyceride-rich lipoprotein particle remodeling, intestinal cholesterol absorption, and plasma lipoprotein particle assembly, as shown in Figure 4C. KEGG analysis indicated significant pathways, including cholesterol metabolism (Figure 4D). To investigate the potential mechanisms activated in GC, GSEA of LINC01094 expression profiles was conducted and the EMT pathway was differentially enriched in the high-LINC01094 expression phenotype (Figure 4E).

The results of GO, KEGG, and GSEA suggest that the tumor microenvironment (TME) may play a key role in LINC01094-related functions. An association between the expression level of LINC01094 and the level of immune cell infiltration quantified by ssGSEA in GC TME was further identified using Spearman's rank correlation. Macrophages were positively correlated with LINC01094 expression significantly with Spearman's rank analysis up to 0.747 with a  $P$ -value less than .001. Other immune cell subsets, including dendritic cells (DCs), immature DCs, activated DCs, Th1 cells, T cells, cytotoxic cells, and Treg cells, were moderately correlated with LINC01094 expression (Figure 5).

A PPI network of LINC01094-associated genes was constructed; the hub genes in the PPI network were extracted using MCODE and found to be involved in various signaling pathways and biological processes, especially the triglyceride-rich lipoprotein particle remodeling and the positive regulation of lipid localization, consistent to the results of GO and KEGG (Figure 6).

Due to the localization of LINC01094 in the cytoplasm, the mediated ceRNA network was constructed. GO enrichment analysis showed that the extracellular structure organization and MHC class II antigen presentation were significantly enriched, and 6 genes, including *FCGR2A*, *PLA2G7*, *SNAI2*, *CTSK*, *VCAN*, and *ADAM12*, were identified based on  $P$ -value  $< .001$  and  $R^2 > 0.6$  using Spearman's rank correlation (Figure 7). *FCGR2A*, *PLA2G7*, *SNAI2*, *CTSK*, and *VCAN* were strongly related to the macrophage infiltration in gastric cancer, and *ADAM12* gene expression was moderately correlated with macrophage infiltration (Figure 8).

## Discussion

Epidemiological studies indicate that Asian countries have a high prevalence of GC. Emerging evidence suggests that genetic factors play a key role in tumorigenesis and cancer progression, which contribute to the high risk of mortality and morbidity of gastric cancer<sup>40</sup>. Thanks to advancements in genomic research, several gastric cancer oncogenes, including *EGFR*,

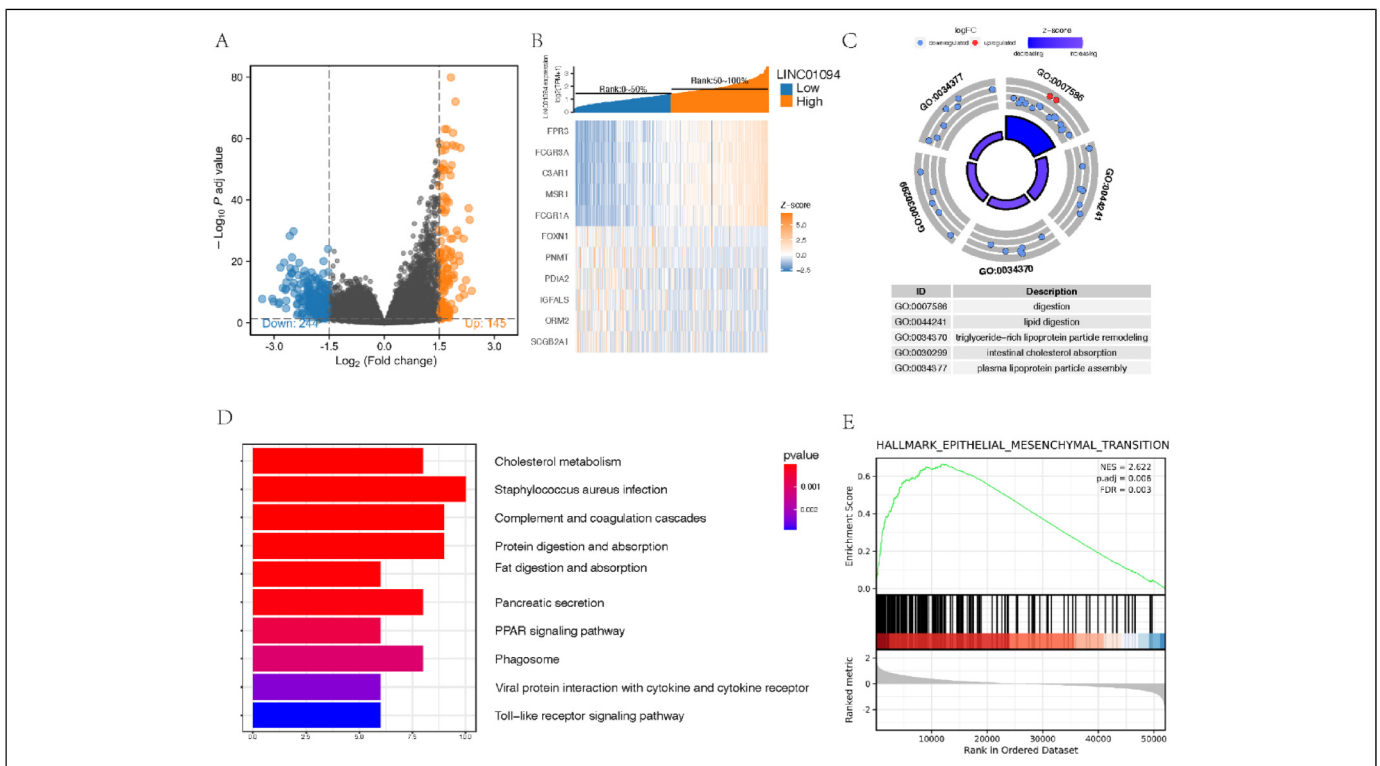


**Figure 4.** (A) Volcano plot of differentially expressed RNAs. Orange and blue represent upregulated and downregulated genes, respectively. (B) Heat map of the top 5 up and down co-expression gene in the TCGA dataset. Enrichment analysis results in GO circle plot (C) using GO analysis and barplot (D) using KEGG analysis. (E) GSEA analysis shows the EMT pathways using hallmark.all.v7.0.symbols.gmt [Hallmarks].



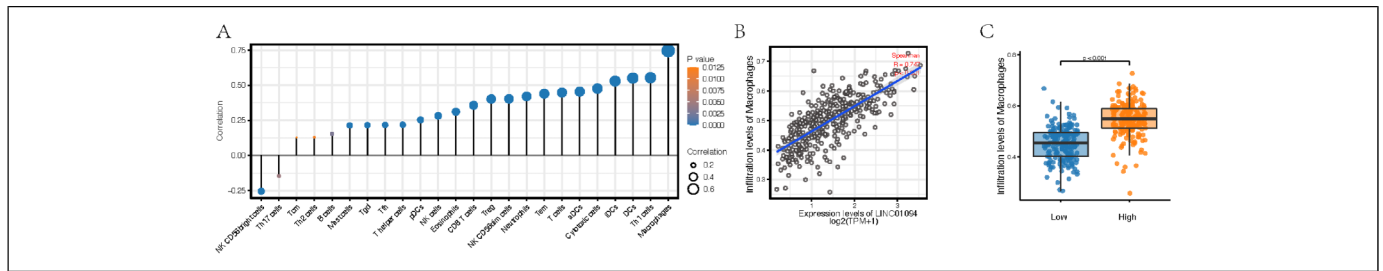


**Figure 5.** The expression level of LINC01094 was associated with the immune infiltration in the tumor microenvironment (A); correlation between the infiltration levels of macrophages and the expression level (TPM) of LINC01094 (B); the difference in macrophage infiltration level between high- and low-LINC01094 expression groups was analyzed by Wilcoxon rank-sum test. The results were statistically significant ( $P < .001$ ) (C).

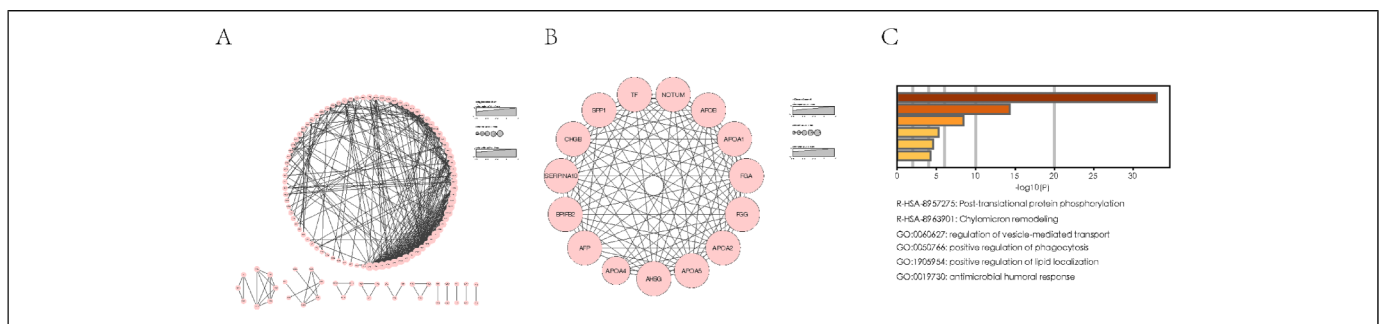


**Figure 6.** (A) Visualized protein–protein interaction (PPI) enrichment analysis of LINC01094-associated genes. (B) The MCODE app selects the key clusters from PPI networks, Mcode score: 14; (C) enrichment analysis of the cluster 1 selected genes.

*HER2*, and K-ras, have been identified and reported. Nevertheless, there is still a need for novel biomarker classes with high specificity, sensitivity, and efficiency for the diagnosis and prognosis of GC.<sup>41</sup>

The role of lncRNAs in malignant tumorigenesis and development has attracted the interests of researchers, as these non-coding RNAs are extensively involved in RNA decoy, epigenetic modification, alternative splicing, and transcriptional or posttranscriptional regulation.<sup>42–44</sup> lncRNAs regulate cell processes to function as tumor boosters or repressors in a wide range of malignancies, including GC.<sup>45–48</sup>

In this study, we revealed that the average expression level of LINC01094 in GC tissues was significantly higher than that in corresponding nontumor tissues. The high expression level of LINC01094 in GC patients was positively correlated with T stage, histologic grade, and pathologic stage. Moreover, high LINC01094 expression in GC tissues was associated with a poor prognosis. In the subgroup analysis, there was a correlation between a poor outcome and high LINC01094 levels in Asian, female, and elderly patients in the early stage. These results suggest that LINC01094 may play an important role in GC progression.

Although LINC01094 has been studied in renal cell carcinoma and glioma, its mechanism in GC remains unclear. In this study, bioinformatic analyses were performed to investigate the function of LINC01094. Based on the gene expression level

in TCGA, we found that LINC01094 was overexpressed in patients with advanced GC. Meanwhile, GSEA pathway analysis of LINC01094 expression profiles suggested it may regulate multiple pathways to promote cancer progression, among which the EMT pathway might be strongly correlated with cancer initiation and metastasis. The progression of EMT is involved in all stages of cancer progression—initiation, primary tumor growth, invasion, dissemination, and metastasis.<sup>49,50</sup> Recent findings have indicated that many lncRNAs demonstrate different functions in different types of EMT and cancer regulation.<sup>51–53</sup> Previous studies have shown that knock-down of LINC01094 increased E-cadherin and decreased N-cadherin levels. LINC01094 insufficiency decreases the levels of Snail family proteins in vitro,<sup>15</sup> suggesting a strong association between LINC01094 and EMT pathways. Additionally, from the LINC01094-associated ceRNA network, we found that the expression levels of the EMT-related genes *SNAIL2* and *VCAN* were highly connected in the ceRNA network. Snail2 is a zinc-finger transcription factor in the Snail family and is widely regarded as a transcription factor for the typical EMT. It plays an essential role in TWIST1-induced EMT and consequently promotes invasion and metastasis.<sup>54</sup> *VCAN*, another EMT-related gene, encodes a large chondroitin sulfate proteoglycan protein that is a major component of the extracellular matrix. Upregulation of *VCAN* can promote leukemia cell invasion through TGF- $\beta$ /

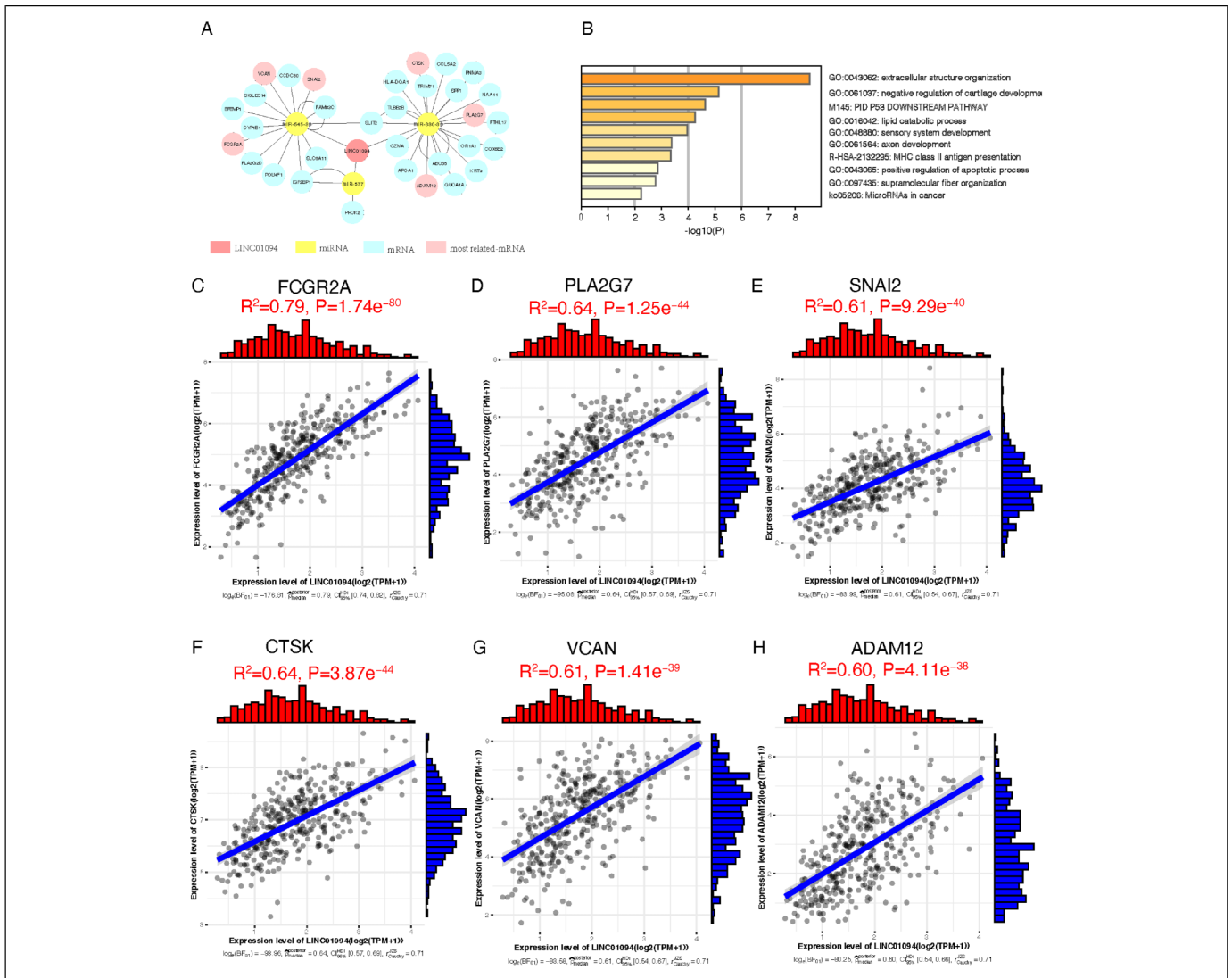


**Figure 7.** (A) Visualized ceRNA network of LINC01094-associated miRNA and mRNA. (B) Enrichment analysis of the LINC01094-associated genes involved in ceRNA. (C-H) Correlations ( $R^2$ ) between LINC01094 and *FCGR2A*, *PLA2G7*, *SNAI2*, *CTSK*, *VCAN*, and *ADAM12* mRNA, which are higher than 0.6.

cPML signaling pathways.<sup>55</sup> Therefore, we suggest that LINC01094 may be involved in the EMT of GC and thus promote tumor invasion and metastasis.

Furthermore, LINC01094 expression was correlated with immune infiltration levels in GC. Our results demonstrated a strong positive relationship between LINC01094 expression and macrophage infiltration levels. Using gene enrichment analysis, LINC01094 was found to be involved in multiple lipid metabolism. Lipid accumulation and metabolism are essential for the differentiation and activation of tumor-associated macrophages (TAMs).<sup>56</sup> TAMs express elevated levels of receptor, accumulate lipids, and use fatty acid oxidation (FAO) for energy instead of glycolysis.<sup>57</sup> TAM infiltration density is associated with recurrence and poor prognosis in various tumors, and it may promote cancer invasion and metastasis through EMT.<sup>58,59</sup> There are also many studies focusing on the

involvement of lncRNAs in tumor development and progression.<sup>60–62</sup> On the other hand, *FCGR2A*, *SNAI2*, *VCAN*, *CTSK*, and *PLA2G7*, the genes in the ceRNA network most related to LINC01094, displayed a similar relationship with macrophage. *FCGR2A* encodes one member of a family of immunoglobulin Fc receptors found on the surface of many immune cells, such as macrophages, and its polymorphisms were always associated with poor clinical outcomes in cancer patients.<sup>63,64</sup> *CTSK* is highly expressed in most cancer, including gastric cancer, and closely related to the infiltration level of immune cells in TME. *PLA2G7* has a similar effect and is associated with aggressive cancer.<sup>65,66</sup> Collectively, these studies support the notion that LINC01094 is closely related to TAM. However, our study still has many shortcomings. Although the experiments described in the literature have illustrated the close association between LINC01094 and other

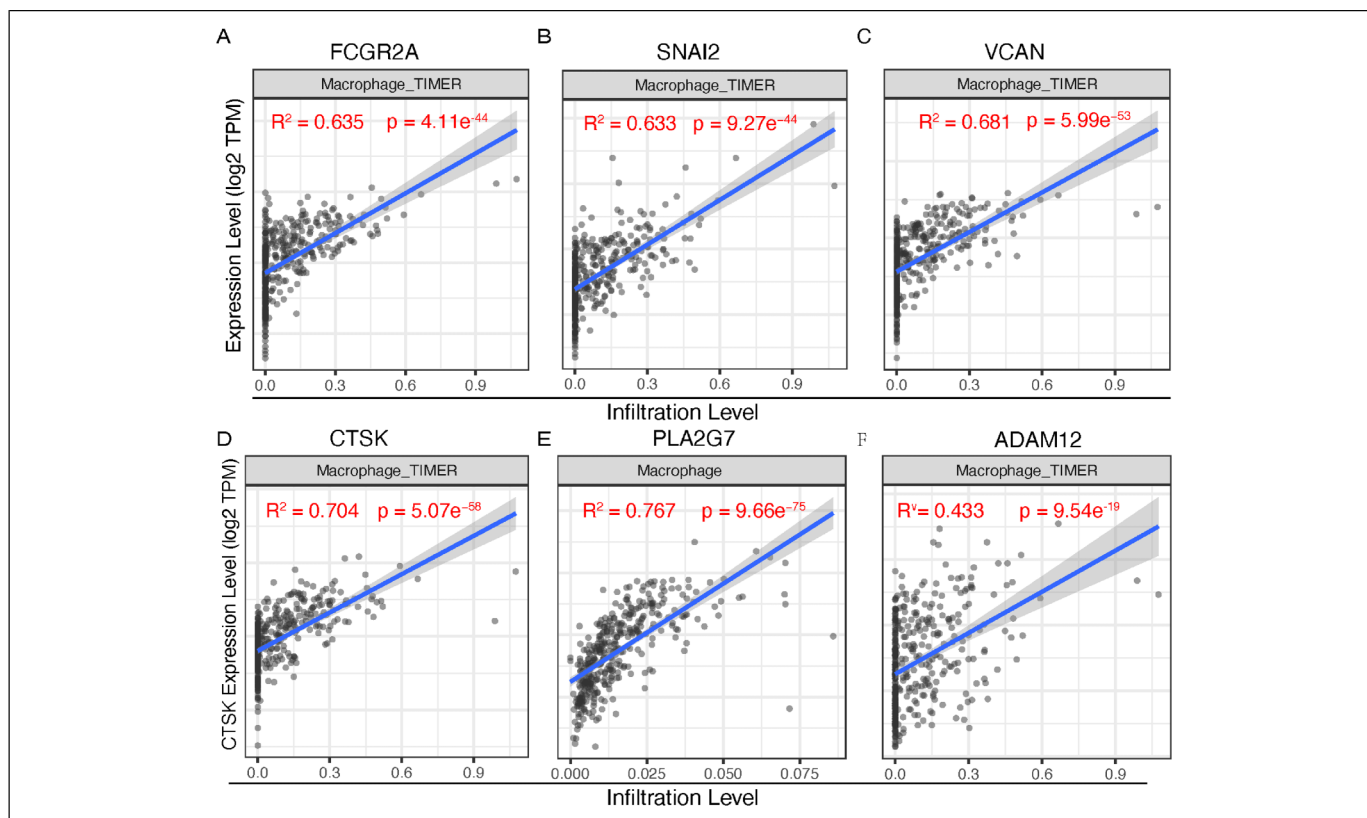


**Figure 8.** (A-F) Correlation between the infiltration levels of macrophages and the expression level (TPM) of *FCGR2A* (A), *SNAI2* (B), *VCAN* (C), *CTSK* (D), *PLA2G7* (E), and *ADAM12* (F).

types of tumors, we have only analyzed its relationship with gastric cancer from a biochemical perspective here. In the future, we will further explore the relationship between the two and the effects of LINC01094 on EMT and TAM infiltration.

## Conclusion

In conclusion, we identified a novel lncRNA, LINC01094, which was upregulated in GC tissue compared to that in the matched normal tissue, and its high expression was associated with GC metastasis and poor OS rates in patients with GC. The EMT pathway and infiltration of macrophages are potential underlying molecular mechanisms.

## Acknowledgments

The authors sincerely appreciated the superb help by Dr. rer. nat. Hao Wu for providing language help, writing assistance, and proofreading the article. And We also acknowledge support from the German Research Foundation (DFG) and the Open Access Publication Fund of Charité - Universitätsmedizin Berlin.

## Ethics in Publishing

In the present study, the tissue microarray was purchased from Shanghai Outdo Biotech Co., Ltd (Shanghai, China) and were approved by the local Ethics Committee (Zhejiang Taizhou Hospital

Ethics Committee, Zhejiang Taizhou Hospital, Zhejiang, China). All the samples were anonymized.


## Declaration of Conflicting Interests

The authors declared no potential conflicts of interest with respect to the research, authorship, and/or publication of this article.

## Funding

The authors disclosed receipt of the following financial support for the research, authorship, and/or publication of this article: This work was supported by the Science and Technology Project of Quanzhou City (grant number 2018N068S).

## ORCID iD

Yuanchun Ye  <https://orcid.org/0000-0002-1514-2605>

## Supplemental Material

Supplemental material for this article is available online.

## References

1. Bray F, Ferlay J, Soerjomataram I, et al. Global cancer statistics 2018: GLOBOCAN estimates of incidence and mortality worldwide for 36 cancers in 185 countries. *CA Cancer J Clin.* 2018;2018(68):394-424. doi: 10.3322/caac.21492.

2. Howlader N, Noone A, Krapcho M, et al. *SEER Cancer Statistics Review, 1975–2017*. National Cancer Institute; 2020.
3. Horii A, Nakatsuru S, Miyoshi Y, et al. The APC gene, responsible for familial adenomatous polyposis, is mutated in human gastric cancer. *Cancer Res.* 1992;52:3231-3233.
4. Hansford S, Kaurah P, Li-Chang H, et al. Hereditary diffuse gastric cancer syndrome: CDH1 mutations and beyond. *JAMA Oncol* 2015;1:23-32. doi: 10.1001/jamaoncol.2014.168.
5. Breast Cancer Linkage C. Cancer risks in BRCA2 mutation carriers. *J Natl Cancer Inst* 1999;91:1310-1316. doi: 10.1093/jnci/91.15.1310.
6. D'Errico M, de Rinaldis E, Blasi MF, et al. Genome-wide expression profile of sporadic gastric cancers with microsatellite instability. *Eur J Cancer* 2009;45:461-469. doi: 10.1016/j.ejca.2008.10.032.
7. Stelzer G, Rosen N, Plaschkes I, et al. The GeneCards suite: from gene data mining to disease genome sequence analyses. *Curr Protoc Bioinformatics* 2016;54:1.30.31-1.30.33. doi: 10.1002/cpbi.5.
8. Li D, Cheng P, Wang J, et al. IRF6 is directly regulated by ZEB1 and ELF3, and predicts a favorable prognosis in gastric cancer. *Front Oncol* 2019;9:220. doi: 10.3389/fonc.2019.00220.
9. Fang Y, Fullwood MJ. Roles, functions, and mechanisms of long non-coding RNAs in cancer. *Genomics Proteomics Bioinformatics* 2016;14:42-54. doi: 10.1016/j.gpb.2015.09.006.
10. Bhan A, Soleimani M, Mandal SS. Long noncoding RNA and cancer: a new paradigm. *Cancer Res* 2017;77:3965-3981. doi: 10.1158/0008-5472.CAN-16-2634.
11. Schmitz SU, Grote P, Herrmann BG. Mechanisms of long non-coding RNA function in development and disease. *Cell Mol Life Sci* 2016;73:2491-2509. doi: 10.1007/s00018-016-2174-5.
12. Huarte M. The emerging role of lncRNAs in cancer. *Nat Med* 2015;21:1253-1261. doi: 10.1038/nm.3981.
13. Li D, She J, Hu X, et al. The ELF3-regulated lncRNA UBE2CP3 is over-stabilized by RNA-RNA interactions and drives gastric cancer metastasis via miR-138-5p/ITGA2 axis. *Oncogene*. 2021;40:5403-5415. doi: 10.1038/s41388-021-01948-6
14. Li CH, Chen Y. Targeting long non-coding RNAs in cancers: progress and prospects. *Int J Biochem Cell Biol* 2013;45:1895-1910. doi: 10.1016/j.biocel.2013.05.030.
15. Jiang Y, Zhang H, Li W, et al. FOXM1-activated LINC01094 promotes clear cell renal cell carcinoma development via microRNA 224-5p/CHSY1. *Mol Cell Biol* 2020;40 (3):e00357-19. doi: 10.1128/MCB.00357-19.
16. Zhu B, Liu W, Liu H, et al. LINC01094 down-regulates miR-330-3p and enhances the expression of MS11 to promote the progression of glioma. *Cancer Manag Res* 2020;12:6511-6521. doi: 10.2147/CMAR.S254630.
17. Jiang Y, Li W, Yan Y, et al. LINC01094 triggers radio-resistance in clear cell renal cell carcinoma via miR-577/CHEK2/FOXM1 axis. *Cancer Cell Int* 2020;20:274. doi: 10.1186/s12935-020-01306-8.
18. Vivian J, Rao AA, Nothaft FA, et al. Toil enables reproducible, open source, big biomedical data analyses. *Nat Biotechnol* 2017;35:314-316. doi: 10.1038/nbt.3772.
19. Tomczak K, Czerwinska P, Wiznerowicz M. The cancer genome atlas (TCGA): an immeasurable source of knowledge. *Contemp Oncol (Pozn)* 2015;19:A68-A77. doi: 10.5114/wo.2014.47136.
20. Liu J, Lichtenberg T, Hoadley KA, et al. An integrated TCGA pan-cancer clinical data resource to drive high-quality survival outcome analytics. *Cell* 2018;173:400-416 e411. doi: 10.1016/j.cell.2018.02.052.
21. Love MI, Huber W, Anders S. Moderated estimation of fold change and dispersion for RNA-seq data with DESeq2. *Genome Biol* 2014;15:550. doi: 10.1186/s13059-014-0550-8.
22. Yu G, Wang LG, Han Y, et al. Cluster profiler: an R package for comparing biological themes among gene clusters. *Omic*s 2012;16:284-287. doi: 10.1089/omi.2011.0118.
23. Damian D, Gorfine M. Statistical concerns about the GSEA procedure. *Nat Genet* 2004;36:663. doi: 10.1038/ng0704-663a.
24. Bindea G, Mlecnik B, Tosolini M, et al. Spatiotemporal dynamics of intratumoral immune cells reveal the immune landscape in human cancer. *Immunity* 2013;39:782-795. doi: 10.1016/j.immuni.2013.10.003.
25. Hanzelmann S, Castelo R, Guinney J. GSEA: gene set variation analysis for microarray and RNA-seq data. *BMC Bioinformatics* 2013;14:7. doi: 10.1186/1471-2105-14-7.
26. Szklarczyk D, Gable AL, Lyon D, et al. STRING V11: protein-protein association networks with increased coverage, supporting functional discovery in genome-wide experimental datasets. *Nucleic Acids Res.* 2019;47:D607-D613. doi: 10.1093/nar/gky1131
27. Bader GD, Hogue CW. An automated method for finding molecular complexes in large protein interaction networks. *BMC Bioinformatics.* 2003;4:2. doi: 10.1186/1471-2105-4-2
28. Shannon P, Markiel A, Ozier O, et al. Cytoscape: a software environment for integrated models of biomolecular interaction networks. *Genome Res* 2003;13:2498-2504. doi: 10.1101/gr.1239303.
29. Zhou Y, Zhou B, Pache L, et al. Metascape provides a biologist-oriented resource for the analysis of systems-level datasets. *Nat Commun* 2019;10:1523. doi: 10.1038/s41467-019-09234-6.
30. Raj A, van den Bogaard P, Rifkin SA, et al. Imaging individual mRNA molecules using multiple singly labeled probes. *Nat Methods.* 2008;5:877-879. doi: 10.1038/Nmeth.1253.
31. Salmena L, Poliseno L, Tay Y, et al. A ceRNA hypothesis: the Rosetta stone of a hidden RNA language? *Cell* 2011;146:353-358. doi: 10.1016/j.cell.2011.07.014.
32. Li JH, Liu S, Zhou H, et al. Starbase v2.0: decoding miRNA-ceRNA, miRNA-ncRNA and protein-RNA interaction networks from large-scale CLIP-Seq data. *Nucleic Acids Res* 2014;42:D92-D97. doi: 10.1093/nar/gkt1248.
33. Ru Y, Kechris KJ, Tabakoff B, et al. The multiMiR R package and database: integration of microRNA-target interactions along with their disease and drug associations. *Nucleic Acids Res* 2014;42: e133. doi: 10.1093/nar/gku631.
34. Patil I. Visualizations with statistical details: The 'ggstatsplot' approach. *Journal of Open Source Software.* 2021;6(61):3167. doi: 10.21105/joss.03167
35. Li T, Fu J, Zeng Z, et al. TIMER2.0 for analysis of tumor-infiltrating immune cells. *Nucleic Acids Res* 2020;48:W509-W514. doi: 10.1093/nar/gkaa407.
36. Chen B, Khodadoust MS, Liu CL, et al. Profiling tumor infiltrating immune cells with CIBERSORT. *Methods Mol Biol* 2018;1711:243-259. doi: 10.1007/978-1-4939-7493-1\_12.

37. Becht E, Giraldo NA, Lacroix L, et al. Estimating the population abundance of tissue-infiltrating immune and stromal cell populations using gene expression. *Genome Biol* 2016;17:218. doi: 10.1186/s13059-016-1070-5.
38. Racle J, de Jonge K, Baumgaertner P, et al. Simultaneous enumeration of cancer and immune cell types from bulk tumor gene expression data. *Elife* 2017;6:e26476. doi: 10.7554/eLife.26476
39. Robin X, Turck N, Hainard A, et al. pROC: an open-source package for R and S+ to analyze and compare ROC curves. *BMC Bioinformatics* 2011;12:77. doi: 10.1186/1471-2105-12-77.
40. Koch L. Cancer genomics: the driving force of cancer evolution. *Nat Rev Genet* 2017;18:703. doi: 10.1038/nrg.2017.95.
41. Matsuoka T, Yashiro M. Biomarkers of gastric cancer: current topics and future perspective. *World J Gastroenterol* 2018;24:2818-2832. doi: 10.3748/wjg.v24.i26.2818.
42. Lee JT. Epigenetic regulation by long noncoding RNAs. *Science* 2012;338:1435-1439. doi: 10.1126/science.1231776.
43. Zhou M, Wang X, Shi H, et al. Characterization of long non-coding RNA-associated ceRNA network to reveal potential prognostic lncRNA biomarkers in human ovarian cancer. *Oncotarget* 2016;7:12598-12611. doi: 10.18632/oncotarget.7181.
44. Choy M, Guo Y, Li H, et al. Long noncoding RNA LOC100129940-N is upregulated in papillary thyroid cancer and promotes the invasion and progression. *Int J Endocrinol* 2019;2019:7043509. doi: 10.1155/2019/7043509.
45. Ding H, Liu J, Zou R, et al. Long non-coding RNA TPTEP1 inhibits hepatocellular carcinoma progression by suppressing STAT3 phosphorylation. *J Exp Clin Cancer Res* 2019;38:189. doi: 10.1186/s13046-019-1193-0.
46. Jia X, Shi L, Wang X, et al. KLF5 regulated lncRNA RP1 promotes the growth and metastasis of breast cancer via repressing p27kip1 translation. *Cell Death Dis* 2019;10(5):373. doi: 10.1038/s41419-019-1566-5
47. Chen X, Chen Z, Yu S, et al. Long noncoding RNA LINC01234 functions as a competing endogenous RNA to regulate CFBF expression by sponging miR-204-5p in gastric cancer. *Clin Cancer Res* 2018;24:2002-2014. doi: 10.1158/1078-0432.CCR-17-2376.
48. Li D, Wang J, Zhang M, et al. LncRNA MAGI2-AS3 is regulated by BRD4 and promotes gastric cancer progression via maintaining ZEB1 overexpression by sponging miR-141/200a. *Mol Ther Nucleic Acids* 2020;19:109-123. doi: 10.1016/j.omtn.2019.11.003.
49. Brabletz T, Kalluri R, Nieto MA, et al. EMT in cancer. *Nat Rev Cancer* 2018;18:128-134. doi: 10.1038/nrc.2017.118.
50. Pastushenko I, Brisebarre A, Sifrim A, et al. Identification of the tumour transition states occurring during EMT. *Nature* 2018;556:463-468. doi: 10.1038/s41586-018-0040-3.
51. Chen DL, Chen LZ, Lu YX, et al. Long noncoding RNA XIST expedites metastasis and modulates epithelial-mesenchymal transition in colorectal cancer. *Cell Death Dis* 2017;8:e3011. doi: 10.1038/cddis.2017.421.
52. Lei H, Gao Y, Xu X. LncRNA TUG1 influences papillary thyroid cancer cell proliferation, migration and EMT formation through targeting miR-145. *Acta Biochim Biophys Sin (Shanghai)* 2017;49:588-597. doi: 10.1093/abbs/gmx047.
53. Liang H, Yu T, Han Y, et al. LncRNA PTAR promotes EMT and invasion-metastasis in serous ovarian cancer by competitively binding miR-101-3p to regulate ZEB1 expression. *Mol Cancer* 2018;17:119. doi: 10.1186/s12943-018-0870-5.
54. Casas E, Kim J, Bendesky A, et al. Snail2 is an essential mediator of Twist1-induced epithelial mesenchymal transition and metastasis. *Cancer Res* 2011;71:245-254. doi: 10.1158/0008-5472.CAN-10-2330.
55. Yang L, Wang L, Yang Z, et al. Up-regulation of EMT-related gene VCAN by NPM1 mutant-driven TGF-beta/cPML signalling promotes leukemia cell invasion. *J Cancer* 2019;10:6570-6583. doi: 10.7150/jca.30223.
56. Wu H, Han Y, Rodriguez Sillke Y, et al. Lipid droplet-dependent fatty acid metabolism controls the immune suppressive phenotype of tumor-associated macrophages. *EMBO Mol Med* 2019;11:e10698. doi: 10.15252/emmm.201910698.
57. Su P, Wang Q, Bi E, et al. Enhanced lipid accumulation and metabolism are required for the differentiation and activation of tumor-associated macrophages. *Cancer Res* 2020;80:1438-1450. doi: 10.1158/0008-5472.CAN-19-2994.
58. Che D, Zhang S, Jing Z, et al. Macrophages induce EMT to promote invasion of lung cancer cells through the IL-6-mediated COX-2/PGE2/beta-catenin signalling pathway. *Mol Immunol* 2017;90:197-210. doi: 10.1016/j.molimm.2017.06.018.
59. Li S, Xu F, Zhang J, et al. Tumor-associated macrophages remodeling EMT and predicting survival in colorectal carcinoma. *Oncoimmunology* 2018;7:e1380765. doi: 10.1080/2162402X.2017.1380765.
60. Liu J, Ding D, Jiang Z, et al. Long non-coding RNA CCAT1/miR-148a/PKCzeta prevents cell migration of prostate cancer by altering macrophage polarization. *Prostate* 2019;79:105-112. doi: 10.1002/pros.23716.
61. Ye Y, Xu Y, Lai Y, et al. Long non-coding RNA Cox-2 prevents immune evasion and metastasis of hepatocellular carcinoma by altering M1/M2 macrophage polarization. *J Cell Biochem* 2018;119:2951-2963. doi: 10.1002/jcb.26509.
62. Li X, Lei Y, Wu M, et al. Regulation of macrophage activation and polarization by HCC-derived exosomal lncRNA TUC339. *Int J Mol Sci* 2018;19(10):2958. doi: 10.3390/ijms19102958
63. Gavin PG, Song N, Kim SR, et al. Association of polymorphisms in FCGR2A and FCGR3A with degree of trastuzumab benefit in the adjuvant treatment of ERBB2/HER2-positive breast cancer: analysis of the NSABP B-31 trial. *JAMA Oncol* 2017;3:335-341. doi: 10.1001/jamaoncol.2016.4884.
64. Zhang W, Gordon M, Schultheis AM, et al. FCGR2A and FCGR3A polymorphisms associated with clinical outcome of epidermal growth factor receptor expressing metastatic colorectal cancer patients treated with single-agent cetuximab. *J Clin Oncol* 2007;25:3712-3718. doi: 10.1200/JCO.2006.08.8021.
65. Lehtinen L, Vainio P, Wikman H, et al. PLA2G7 associates with hormone receptor negativity in clinical breast cancer samples and regulates epithelial-mesenchymal transition in cultured breast cancer cells. *J Pathol Clin Res* 2017;3:123-138. doi: 10.1002/cjp.2.69.
66. Vainio P, Lehtinen L, Mirtti T, et al. Phospholipase PLA2G7, associated with aggressive prostate cancer, promotes prostate cancer cell migration and invasion and is inhibited by statins. *Oncotarget* 2011;2:1176-1190. doi: 10.18632/oncotarget.397.